IEEE Robotics and Automation Letters (RA-L) paper, presented at ICRA 2026, Vienna, Austria. Cite as RA-L paper.

Distributed Bearing-only Formation Maneuvering Control for Quadrotors without Global Reference Frame

Shaoshi Li, Yuwei Zhang, Shaoping Wang, Rui Mu, and Xingjian Wang

***Abstract*—Most existing bearing-only formation control methods required that the relative bearings among neighboring agents are measured under a well-known global reference frame for each individual. To remove such constraint, this paper novelly introduces a distributed formation control scheme for quadrotors with only bearing measurement in each vehicle's local reference frame. To this end, firstly, a prescribed-time quaternion-based orientation estimator is proposed for each follower to estimate the leader's orientation without knowledge of the global reference frame. Secondly, a bearing-only formation control law is developed to achieve desired maneuvering formation using relative bearings under local reference frame, wherein a finite-time differentiator is incorporated to remove the need of bearing rate. The convergence is rigorously proven through mathematical derivations. Both comparative simulations and real-world experiments are conducted to validate the effectiveness of the proposed control scheme.**

***Index Terms*—Bearing-only measurement, formation control, orientation estimation, quadrotor swarm**

I. Introduction

Recent advances in coordination control have enhanced the autonomy and agility of UAVs, enabling their deployment in diverse environments for tasks such as area monitoring [1], cooperative transportation [2], and source seeking [3]. Formation control, a key topic in cooperative control, aims to align multiple UAVs into and maintain a desired geometric configuration during flight.

Depending on the measurement requirements to achieve the target formation, the existing formation control methods can be primarily categorized into three types: displacement-based [4], distance-based [5], and bearing-based [6], [7]. Different from the first two methods, bearing-based control leverages relative bearing information to achieve the formation, which can be obtained using passive sensors like low-cost vision camera, therefore reducing the sensing requirements for UAVs. Additionally, a formation control law is termed *bearing-only* if it relies solely on bearing information, without displacement or distance measurements between neighboring agents [8].

Bearing-only control has attracted significant attention due to its advantages, leading to substantial progress in recent years. A foundational work [8] introduced bearing rigidity theory to characterize formation uniqueness, enabling controller design for formations with stationary leaders. Subsequent studies addressed practical challenges such as disturbances [9], heterogeneity [10], predefined convergence [11], and fault tolerance [12]. For moving formations, control laws under constant leader velocity have been developed [13]. However, with time-varying leader velocity, bounded bearing errors cannot prevent unbounded position errors [14], risking divergence unless gains are large or motion is slow. A recent work [15] addressed this by proposing a bearing-only controller for time-varying velocities.

Nonetheless, existing formation control laws often assume that bearing vectors are measured in a common global reference frame, which is impractical in distributed settings where only local frames are available [16]. To overcome this, orientation estimation or synchronization is typically performed prior to control, eliminating the need for global frame measurements. For example, [17] proposes a bearing-only control protocol using local elevation angles. However, these methods lack explicit guarantees on estimation time and are limited in handling time-varying formation velocities and external disturbances.

Motivated by the above discussions, this paper addresses bearing-only formation control for quadrotors, where each UAV relies on body-fixed bearing measurements. The sensing topology among the quadrotors is represented by a specifically defined directed graph. A prescribed-time orientation estimation method is introduced to acquire orientation information within a user-defined time. Then, a bearing-only formation control law is proposed to achieve the desired formation in the local coordinate frame while maneuvering with time-varying velocities. The main contributions of this research can be summarized as follows:

- The proposed control scheme derives the relative orientation of each UAV with respect to the leader through prescribed time-based orientation estimation, without knowledge of the global reference frame. As a result, it is better suited to meet the requirements of distributed control in GNSS-denied environment compared to existing approaches such as [18].
- The proposed bearing-only formation control law requires only local bearing information which can be passively measured with low-cost sensors. Compared with [17], the practicability is improved as it reduces the quadrotor's

Manuscript received: July 30, 2025; revised October 3, 2025; Accepted: November 19, 2025.

This paper was recommended for publication by Editor M. Ani Hsieh upon evaluation of the Associate Editor and Reviewers' comments. This work is supported in part by the National Natural Science Foundation of China (Grant Nos. 62303030, 62403028, 52275044 and U2233212), the Zhejiang Provincial Natural Science Foundation of China (Grant No. LZ23E050006), the Postdoctoral Fellowship Program of CPSF (Grant no. GZC20233377) and the Fundamental Research Funds for the Central Universities. *(Corresponding authors: Yuwei Zhang and Rui Mu.)*

S. Li, Y, Zhang, S. Wang, R. Mu and X. Wang are with School of Automation Science and Electrical Engineering, Beihang University, Beijing 100191, China.

Y, Zhang is also with the National Key Laboratory of Aircraft Integrated Flight Control, Beijing 100191, China.

Digital Object Identifier (DOI): see top of this page.

IEEE Robotics and Automation Letters (RA-L) paper, presented at ICRA 2026, Vienna, Austria. Cite as RA-L paper.

sensing requirement such as position, velocity, or bearing rate.
- The time-varying desired velocity and disturbance are handled simultaneously with the proposed bearing-only formation control law, which contrasts with existing bearing-only formation control scheme [13], [19] where the desired formation velocity is restricted to be constant.

The remainder of the paper is organized as below. Section II introduces some preliminaries and formulates the problem. Section III presents the proposed bearing-only formation control scheme. Section IV illustrates the effectiveness of the proposed method through comparative simulations. In Section V, the control scheme is validated with multiple quadrotors in real-world environment, after which the conclusions are drawn.

II. Preliminaries and Problem Formulation

Notations: Let $\mathbb{R}^d$ denote the d-dimensional Euclidean space and $\boldsymbol{I}_d$ the $d \times d$ identity matrix. $\odot$ is the quaternion multiplication. The 1- and 2-norm of a vector or matrix are denoted by $\|\cdot\|_1$ and $\|\cdot\|$, respectively. For a vector $\boldsymbol{x} = [x_1, \ldots, x_n]^T \in \mathbb{R}^n$, $\mathrm{sgn}(\boldsymbol{x}) = [\mathrm{sgn}(x_1), \ldots, \mathrm{sgn}(x_n)]^T$ with $\mathrm{sgn}(\cdot)$ as the signum function. The skew-symmetric matrix corresponding to $\boldsymbol{\omega} = [\omega_x, \omega_y, \omega_z]^T \in \mathbb{R}^3$ is $[\boldsymbol{\omega}]_\times = [0, -\omega_z, \omega_y; \omega_z, 0, -\omega_x; -\omega_y, \omega_x, 0]$. The n-dimensional unit sphere embedded in $\mathbb{R}^{n+1}$ is denoted as $\mathbb{S}^n = \{\boldsymbol{x} \in \mathbb{R} \times \mathbb{R}^n | \boldsymbol{x}^T\boldsymbol{x} = 1\}$.

A. Unit Quaternion

Consider a quaternion $\boldsymbol{q} = [\eta, \boldsymbol{\varepsilon}^T]^T$ consisting of the scalar part $\eta \in \mathbb{R}$ and vector part $\boldsymbol{\varepsilon} \in \mathbb{R}^3$. A unit quaternion $\boldsymbol{q}$ satisfies that $\boldsymbol{q}^T\boldsymbol{q} = 1$. The quaternion multiplication of two quaternions $\boldsymbol{q}_i = [\eta_i, \boldsymbol{\varepsilon}_i^T]^T$ and $\boldsymbol{q}_j = [\eta_j, \boldsymbol{\varepsilon}_j^T]^T$ is defined as

$$\boldsymbol{q}_i \odot \boldsymbol{q}_j = \begin{bmatrix} \eta_i\eta_j - \boldsymbol{\varepsilon}_i^T\boldsymbol{\varepsilon}_j \\ \eta_i\boldsymbol{\varepsilon}_j + \eta_j\boldsymbol{\varepsilon}_i + [\boldsymbol{\varepsilon}_i]_\times\boldsymbol{\varepsilon}_j \end{bmatrix} \tag{1}$$

According to [20], the rotation from the inertial frame Σ_I to the body frame of the ith quadrotor Σ_i can be represented by a unit quaternion q. The corresponding rotation matrix from Σ_i to Σ_I is $\boldsymbol{R}_i = \boldsymbol{R}(\boldsymbol{q}_i) = (\eta_i^2 - \boldsymbol{\varepsilon}_i^T\boldsymbol{\varepsilon}_i)\boldsymbol{I}_3 + 2\eta_i[\boldsymbol{\varepsilon}_i]_\times + 2\boldsymbol{\varepsilon}_i\boldsymbol{\varepsilon}_i^T$. The angular velocity of the rotation is denoted as Σ_i as ω_i. And the rotation kinematics is expressed as $\dot{\boldsymbol{q}}_i = \boldsymbol{G}(\boldsymbol{q}_i)\boldsymbol{\omega}_i/2$, where $\boldsymbol{G}(\boldsymbol{q}_i) = [-\boldsymbol{\varepsilon}_i^T, \eta_i\boldsymbol{I}_3 + [\varepsilon_i]_\times]^T$.

Let two quaternions $\boldsymbol{q}_i$ and $\boldsymbol{q}_j$ represent the rotation from the inertial frame to body frames of two different quadrotors i and j. And the corresponding angular velocities are $\boldsymbol{\omega}_i$ and $\boldsymbol{\omega}_j$. The quaternion error is defined as $\boldsymbol{q}_{ij} = \boldsymbol{q}_j^{-1} \odot \boldsymbol{q}_i$. Furthermore, the derivative of $\boldsymbol{q}_{ij}$ is $\dot{\boldsymbol{q}}_{ij} = \boldsymbol{G}(\boldsymbol{q}_{ij})\boldsymbol{\omega}_{ij}/2$ with $\boldsymbol{G}(\boldsymbol{q}_{ij}) = [-\boldsymbol{\varepsilon}_{ij}^T, \eta_{ij}\boldsymbol{I}_3 + [\varepsilon_{ij}]_\times]^T$.

B. Quadrotor Dynamics

Consider the following translational dynamics for quadrotor

$$\begin{cases} \dot{\boldsymbol{p}}_i = \boldsymbol{v}_i, \\ m_i\dot{\boldsymbol{v}}_i = -T_i\boldsymbol{R}_i\boldsymbol{e}_3 + m_ig\boldsymbol{e}_3 + \boldsymbol{d}_i \\ \qquad = -T_i\left(\boldsymbol{R}_i\boldsymbol{e}_3 - \boldsymbol{R}_i^*\boldsymbol{e}_3\right) - T_i\boldsymbol{R}_i^*\boldsymbol{e}_3 + m_ig\boldsymbol{e}_3 + \boldsymbol{d}_i \end{cases} \tag{2}$$

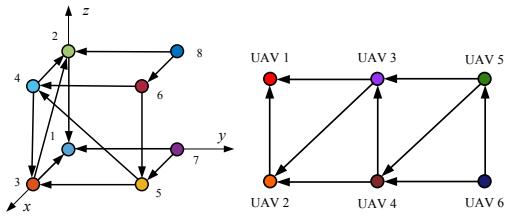

(a) (b)

Fig. 1. Examples of LFF structure: (a) Communication topology for quadrotors in simulation; (b) Communication topology for quadrotors in experiment.

where m_i is the mass of the quadrotor. $\boldsymbol{R}_i$ is the rotation matrix from the inertial frame to the body-fixed frame, and $\boldsymbol{R}_i^*$ is the desired rotation matrix defining the desired UAV orientation. $\boldsymbol{e}_3 = [0, 0, 1]^T$. Utilizing the time-scale separation assumption that the attitude control is typically designed to achieve sufficiently fast convergence than the velocity control, it can be assumed that the rotation matrix can rapidly track its desired value, i.e., $\boldsymbol{R}_i \to \boldsymbol{R}_i^*$, during the evolution of the velocity dynamics [21]–[23]. Therefore, (2) can be simplified as

$$\begin{cases} \dot{\boldsymbol{p}}_i = \boldsymbol{v}_i \\ \dot{\boldsymbol{v}}_i = \boldsymbol{u}_i + \boldsymbol{d}_i \end{cases} \tag{3}$$

where $\boldsymbol{u}_i = -T_i\boldsymbol{R}_i\boldsymbol{e}_3/m_i + g\boldsymbol{e}_3$ is the virtual control input. The thrust force T_i can be calculated by $T_i = m_i\|\boldsymbol{u}_i - g\boldsymbol{e}_3\|$. The z-axis for quadrotor i is set as $\boldsymbol{r}_{3,i} = (\boldsymbol{u}_i - g\boldsymbol{e}_3)/\|\boldsymbol{u}_i - g\boldsymbol{e}_3\|$.

Remark 1. *Since $\boldsymbol{u}_i$ is defined in the inertial frame, the thrust vector $-T_i\boldsymbol{r}_{3,i}$ should align with $m_i(\boldsymbol{u}_i - g\boldsymbol{e}_3)$ to realize the desired acceleration. Specifically, $\boldsymbol{r}_{3,i}$ is determined by normalizing $(\boldsymbol{u}_i - g\boldsymbol{e}_3)$, and T_i is given by its magnitude. This establishes a clear physical link between the simplified translational dynamics and the actual quadrotor attitude: the desired acceleration in the inertial frame uniquely determines both the thrust magnitude and the orientation of the body-z axis through $\boldsymbol{R}_i$.*

C. Quadrotor swarm with Leader-first Follower Structure

Consider a quadrotor swarm of n agents in $\mathbb{R}^3$, where the sensing and communication topology is modeled by a directed graph $\mathcal{G} = \{\mathcal{V}, \mathcal{E}\}$. Here, $\mathcal{V} = \{v_1, v_2, \ldots, v_n\}$ represents UAVs, and $\mathcal{E} = \{(v_i, v_j)\}$ represents communication links. A directed edge $(v_i, v_j) \in \mathcal{E}$ indicates that quadrotor j can sense the relative bearing of quadrotor i. The neighbor set of quadrotor i is $\mathcal{N}_i = \{j \in \mathcal{V} \mid (v_i, v_j) \in \mathcal{E}\}$.

With the above relationship between the sensing and communication topology and directed graph $\mathcal{G}$, the formation configuration of the quadrotor swarm can be defined as $(\mathcal{G}, \boldsymbol{p})$, where $\boldsymbol{p} = [\boldsymbol{p}_1^T, \boldsymbol{p}_2^T, \cdots, \boldsymbol{p}_n^T]^T$ is the stacked position vector of the formation. For each directed edge $(v_j, v_i) \in \mathcal{E}$, the edge vector is given as $\boldsymbol{e}_{ij} = \boldsymbol{p}_j - \boldsymbol{p}_i$, and the bearing vector is defined as $\boldsymbol{g}_{ij} = \boldsymbol{e}_{ij}/\|\boldsymbol{e}_{ij}\|$, where $\|\boldsymbol{e}_{ij}\|$ is the 2-norm of $\boldsymbol{e}_{ij}$. It can be seen that $\boldsymbol{g}_{ij}$ is unit vector representing the bearing from $\boldsymbol{p}_i$ to $\boldsymbol{p}_j$. Noting that $\boldsymbol{g}_{ij}$ is a unit vector, the orthogonal projection matrix of $\boldsymbol{g}_{ij}$ can be defined as $\boldsymbol{P}_{ij} = \boldsymbol{I}_3 - \boldsymbol{g}_{ij}\boldsymbol{g}_{ij}^T$. Moreover, the time derivative of $\boldsymbol{g}_{ij}$ is $\dot{\boldsymbol{g}}_{ij} = \boldsymbol{P}_{ij}\dot{\boldsymbol{e}}_{ij}/\|\boldsymbol{e}_{ij}\|$.

IEEE Robotics and Automation Letters (RA-L) paper, presented at ICRA 2026, Vienna, Austria. Cite as RA-L paper.

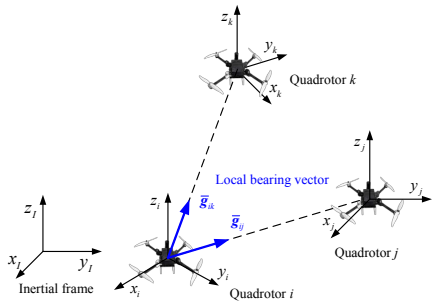

Fig. 2. Relative bearing measurement for quadrotor i with neighbors j, k.

In bearing-based formation control, only bearing constraints $\Gamma = \{\boldsymbol{g}_{ij}^* | (v_j, v_i) \in \mathcal{E}\}$ is provided, where $\boldsymbol{g}_{ij}^*$ is the desired bearing vector. Therefore, the uniqueness of the bearing-constrained formation is the primary problem for bearing-based formation control. Motivated by [24], a specific directed graph named leader-first follower structure (LFF) is investigated in this paper:

Definition 1. *[24] A directed and acyclic graph is named to be LFF structure if it has n vertices and $2n-3$ properly selected directed edges, which satisfies the following conditions:*

- *The n vertices include one leader, one first follower and $n-2$ followers;*
- *The first follower has the leader as its only neighbor, and each follower has precisely two neighbors.*

Some examples of LFF structure are illustrated in Fig. 1. Without loss of generality, it is assumed that v_1 is the leader with $\mathcal{N}_1 = \emptyset$, v_2 is the first follower with $\mathcal{N}_2 = \{v_1\}$ and v_i $(i = 3, \cdots, n)$ is the follower with $\mathcal{N}_i = \{v_j, v_k\}$ $(j < k < i \leq n)$. The uniqueness of the LFF structure is given by the following lemma :

Lemma 1. *[24] With the bearing constraints Γ and positions of the leader $\boldsymbol{p}_1$ and first follower $\boldsymbol{p}_2$, the desired formation configuration $(\mathcal{G}, \boldsymbol{p}^*)$ with $\boldsymbol{p}^* = [(\boldsymbol{p}_1^*)^T, (\boldsymbol{p}_2^*)^T, \cdots, (\boldsymbol{p}_n^*)^T]^T$ can be uniquely determined if the following conditions are satisfied: 1) The desired bearing constraints are achievable, i.e., there exists formation configuration $(\mathcal{G}, \boldsymbol{p})$ such that $\boldsymbol{g}_{ij} = \boldsymbol{g}_{ij}^*$ for $(v_j, v_i) \in \mathcal{E}$; 2) The desired bearing constraints between each follower and its two neighbors are not collinear, i.e., $\boldsymbol{g}_{ij}^* \neq \pm \boldsymbol{g}_{ik}^*$.*

On this basis, the desired position of follower i can be calculated by $\boldsymbol{p}_i^* = \boldsymbol{M}_i^{-1} \sum_{j \in \mathcal{N}_i} \boldsymbol{P}_{ij}^* \boldsymbol{p}_j^*$, where $\boldsymbol{M}_i = \sum_{j \in \mathcal{N}_i} \boldsymbol{P}_{ij}^*$.

D. Problem Formulation

As illustrated in Fig. 2, this paper investigates the bearing-only formation control problem for quadrotors without knowledge of inertial frame. To address such issue, we employ the leader' s attitude (denoted by $\boldsymbol{q}_r$) as the common frame. If each UAV can align its attitude with the leader, the local bearing vector will be given by $\bar{\boldsymbol{g}}_{ij} = \boldsymbol{R}(\boldsymbol{q}_r)\boldsymbol{g}_{ij}$. Therefore, each UAV only needs to estimate the leader's attitude, no inertial frame is required.

For a group of quadrotors modeled as (3), the virtual control input $\boldsymbol{u}_i$ is designed accordingly for each follower to maintain the desired bearing constraints Γ while maneuvering. Moreover, the desired formation is achieved if the position tracking error $\boldsymbol{e}_{pi} = \boldsymbol{p_i} - \boldsymbol{p}_i^*$ and velocity tracking error $\boldsymbol{e}_{vi} = \boldsymbol{v_i} - \boldsymbol{v}_i^*$ converge to zero.

Before formulating the problem, the following assumptions are made:

Assumption 1. *The communication network of the quadrotor swarm satisfies the LFF structure.*

Assumption 2. *The leader and the first follower are at their desired trajectories, i.e., $\boldsymbol{p}_i(t) = \boldsymbol{p}_i^*(t)$ and $\boldsymbol{R}(\boldsymbol{q}_i) = \boldsymbol{R}(\boldsymbol{q}_r)$ for $i = 1, 2$. The accelerations of the leader and first follower satisfy $\|\ddot{\boldsymbol{p}}_i\| \leq \xi_a$, where ξ_a is a positive constant.*

Assumption 3. *The external disturbance is bounded and satisfies that $\|\boldsymbol{d}_i\| \leq \xi_d$, where ξ_d is a positive constant.*

Remark 2. *Under the standard time-scale separation assumption between attitude and translational dynamics [21]–[23], the term $\boldsymbol{d}_i$ in (3) can be regarded as an unknown but bounded disturbance. However, if the attitude control loop is not sufficiently fast or is affected by external disturbances, the actual rotation matrix $\boldsymbol{R}_i$ may deviate from its desired value $\boldsymbol{R}_i^*$, introducing additional coupling effects that may degrade tracking performance or even affect stability. Nevertheless, the upper bound of $\boldsymbol{d}_i$ can be estimated empirically through CFD simulations or wind tunnel experiments [25].*

The bearing-only formation maneuvering control problem for quadrotors can be formulated as follows:

Problem 1 (Prescribed-time quadrotors orientation estimation)**.** *Consider a group of quadrotors with LFF structure, under Assumption 1-3, given the leader trajectories $\boldsymbol{p}_i^*$ $(i = 1, 2)$ and bearing constraints Γ, design orientation estimation $\hat{\boldsymbol{R}}_i$ for each follower quadrotor, such that the orientation estimation error $\boldsymbol{e}_{Ri} = \hat{\boldsymbol{R}}_i - \boldsymbol{R}(\boldsymbol{q}_r)$ converges to zero within prespecified time T_{qi}.*

Problem 2 (Bearing-only quadrotors formation maneuvering control)**.** *Consider a group of quadrotors with LFF structure, under Assumption 1-3, given the leader trajectories $\boldsymbol{p}_i^*$ $(i = 1, 2)$ and bearing constraints Γ, designed control input $\boldsymbol{u}_i$ for each follower quadrotor based on the local bearing measurement and orientation estimation, such that the position tracking error $\boldsymbol{e}_{pi}$ and velocity tracking error $\boldsymbol{e}_{vi}$ converge to zero asymptotically.*

III. Main Results

In this section, a distributed control scheme is proposed to solve Problems 1 and 2. A prescribed-time quaternion-based orientation estimator is first designed to obtain the desired orientation within a finite time. Based on this estimate, a bearing-only formation controller is developed to achieve maneuvering with time-varying velocities.

A. Prescribed-time Orientation Estimation Design

Motivated by [26], a prescribed-time scaling function is introduced as

$$\xi(t) = \begin{cases} \frac{T_c^h}{(t_s + T_c - t)^h} & t \in [t_s, t_e) \\ 1 & t \in [t_e, +\infty) \end{cases} \tag{4}$$

IEEE Robotics and Automation Letters (RA-L) paper, presented at ICRA 2026, Vienna, Austria. Cite as RA-L paper.

where t_s and t_e are the start time and end time of the prescribed-time convergence. $T_c = t_e - t_s$, $h > 0$. The derivative of $\xi(t)$ is:

$$\dot{\xi}(t) = \begin{cases} \frac{h}{T_c}\xi^{1+\frac{1}{h}} & t \in [t_s, t_e) \\ 0 & t \in [t_e, +\infty) \end{cases} \tag{5}$$

The following lemma of prescribed-time convergence is introduced before presenting the orientation estimator:

Lemma 2. *[26] Consider a system $\dot{x}(t) = f(t, x(t)), t \in \mathbb{R}^+, x(0) = x_0$ and a continuously differentiable function $V : \mathcal{U} \times \mathbb{R}^+ \to \mathbb{R}$, where $\mathcal{U} \subset \mathbb{R}^m$ is a domain containing the origin, if there exist $a, b \in \mathbb{R}^+$ such that in $t \in [t_0, +\infty)$, $\dot{V} \leq -aV - b\frac{\dot{\xi}}{\xi}V$, where $\xi(t)$ is given as 4, then it yields that:*

$$V(t) \begin{cases} \leq \mu^{-b} e^{-a(t-t_0)} V(t_0), & t \in [t_0, t_1) \\ \equiv 0, & t \in [t_1, +\infty) \end{cases} \tag{6}$$

where $\dot{V} = (\partial V/\partial x) f(t, x)$. The origin of system $\dot{x}(t)$ is prescribed-time stable with the prescribed time T_c given in (5).

For the ith quadrotor ($3 \leq i \leq n$), the estimation of $\boldsymbol{q}_i = [\eta_i, \boldsymbol{\varepsilon}_i^T]^T$ is defined as $\hat{\boldsymbol{q}}_i = [\hat{\eta}_i, \hat{\boldsymbol{\varepsilon}}_i^T]^T$. Considering $\hat{\boldsymbol{q}}_1 = \hat{\boldsymbol{q}}_2 = \boldsymbol{q}_r$ and $\hat{\boldsymbol{\omega}}_1 = \hat{\boldsymbol{\omega}}_2 = \hat{\boldsymbol{\omega}}_r$ as $\boldsymbol{q}_r$ and $\boldsymbol{\omega}_r$ are directly available to the leader and first follower. Therefore, the prescribed-time distributed orientation observer is designed as

$$\begin{cases} \dot{\hat{\boldsymbol{q}}}_i = \frac{1}{2} G(\hat{\boldsymbol{q}}_i)\hat{\boldsymbol{\omega}}_i \\ \hat{\boldsymbol{\omega}}_i = \frac{1}{2}\left(\sum_{j\in\mathcal{N}_i} \boldsymbol{R}_{ij}^T \hat{\boldsymbol{\omega}}_j - \kappa_i \boldsymbol{\varepsilon}_{ij}\right) \end{cases} \tag{7}$$

where $\boldsymbol{R}_{ij} = \boldsymbol{R}(\boldsymbol{q}_{ij})$ is the corresponding rotation matrix of the quaternion error $\boldsymbol{q}_{ij} = \hat{\boldsymbol{q}}_j^{-1} \odot \hat{\boldsymbol{q}}_i$, and $\boldsymbol{\varepsilon}_{ij}$ is the vector part of $\boldsymbol{q}_{ij}$. κ_i is the prescribed-time scaling function defined as $\kappa_i = a_i + b_i \dot{\xi}_i / \xi_i$, where $a_i \in \mathbb{R}^+$, $b_i > 4$. The prescribed convergence time for ξ_i is T_{qi}.

Remark 3. *The distributed observer (7) estimates the leader's orientation $\boldsymbol{q}_r$, which can be defined in any reference frame. For example, setting $\boldsymbol{q}_r = [1, 0, 0, 0]^T$ aligns the swarm with the leader's frame, while expressing $\boldsymbol{q}_r$ in the inertial frame aligns all UAVs accordingly. This flexibility is advantageous in GNSS-denied environments, where the inertial frame may be unavailable, allowing the swarm to operate in the leader's coordinate system.*

Theorem 1. *Consider a group of n quadrotors, suppose that Assumptions 1-3 holds, if the initial estimation $\hat{\boldsymbol{q}}_i(0)$ satisfies that $\hat{\boldsymbol{q}}_i(0) \in \mathbb{S}^3$, the orientation estimation law (7) guarantees that $\hat{\boldsymbol{q}}_i \to \boldsymbol{q}_r$ and $\hat{\boldsymbol{\omega}}_i \to \boldsymbol{\omega}_r$ for $3 \leq i \leq n$ within prescribed convergence time T_{qi}.*

Proof. The proof will be conducted using mathematical induction. We firstly consider the third quadrotor ($i = 3$) with the leader ($j = 1$) and first follower ($k = 2$) as its neighbors. The quaternion estimation error of the quadrotor i is defined as $\tilde{\boldsymbol{q}}_i = \boldsymbol{q}_r^{-1} \odot \hat{\boldsymbol{q}}_i$. According to Assumption 2, we have $\hat{\boldsymbol{q}}_j = \hat{\boldsymbol{q}}_k = \boldsymbol{q}_r$, thus it yields that $\tilde{\boldsymbol{q}}_i = \boldsymbol{q}_{ij} = \boldsymbol{q}_{ik}$.

The derivative of $\tilde{\boldsymbol{q}}_i = [\tilde{\eta}_i, \tilde{\boldsymbol{\varepsilon}}_i^T]^T$ is $\dot{\tilde{\boldsymbol{q}}}_i = \frac{1}{2}\boldsymbol{G}(\tilde{\boldsymbol{q}}_i)(\hat{\boldsymbol{\omega}}_i - \boldsymbol{R}^T(\tilde{\boldsymbol{q}}_i)\boldsymbol{\omega}_r) = -\frac{\kappa_i}{2}\boldsymbol{G}(\tilde{\boldsymbol{q}}_i)\tilde{\boldsymbol{\varepsilon}}_i$, where $\tilde{\boldsymbol{\varepsilon}}_i$ is the vector part of $\tilde{\boldsymbol{q}}_i$.

Consider the Lyapunov function candidate $V_{qi} = 2(1 - \tilde{\eta}_i)$. As $\tilde{\boldsymbol{q}}_i$ is unit quaternion, we have $V_{qi} \geq 0$. The derivative of V_{qi} is $\dot{V}_{qi} = -\kappa_i \tilde{\boldsymbol{\varepsilon}}_i^T \tilde{\boldsymbol{\varepsilon}}_i \leq 0$.

As $\tilde{\boldsymbol{q}}_i$ is unit quaternion, it can be obtained that $(1 - \tilde{\eta}_i)^2 \leq (1 - \tilde{\eta}_i)(1 + \tilde{\eta}_i) = \tilde{\boldsymbol{\varepsilon}}_i^T \tilde{\boldsymbol{\varepsilon}}_i$.

Therefore, V_{qi} can be rewritten as $V_{qi} = 1 - 2\tilde{\eta}_i + \tilde{\eta}_i^2 + \tilde{\boldsymbol{\varepsilon}}_i^T \tilde{\boldsymbol{\varepsilon}}_i == \tilde{\boldsymbol{\varepsilon}}_i^T \tilde{\boldsymbol{\varepsilon}}_i + (1 - \tilde{\eta}_i)^2 \leq 2\tilde{\boldsymbol{\varepsilon}}_i^T \tilde{\boldsymbol{\varepsilon}}_i$, which yields that $\dot{V}_{qi} \leq -\frac{\kappa_i}{2} V_{qi}$. According to Lemma 2, it is proven that $\tilde{\eta}_i \to 1$ and $\tilde{\boldsymbol{\varepsilon}}_i \to \boldsymbol{0}$ in prescribed time T_{qi}. Therefore, it is concluded that $\boldsymbol{R}_{ij} = \boldsymbol{I}_3$ in $t \geq T_{qi}$, which means that $\hat{\boldsymbol{R}}_i \to \boldsymbol{R}(\boldsymbol{q}_r)$ in T_{qi} for $i = 3$ and ends the proof for the quadrotor 3.

For follower quadrotor i ($3 < i \leq n$) with neighbor quadrotors j and k, we assume that the claim holds until $i-1$. Therefore, due to the LFF structure, we have $k < j < i$, which means that $\hat{\boldsymbol{q}}_j = \boldsymbol{q}_r$ and $\hat{\boldsymbol{q}}_k = \boldsymbol{q}_r$ in $t \in [T_{qk}, +\infty)$. Similar to the above proof, it can be concluded that $\hat{\boldsymbol{R}}_i \to \boldsymbol{R}(\boldsymbol{q}_r)$ in prescribed time T_{qi} for $3 \leq i \leq n$. Therefore, it can be concluded that the orientation estimation for each follower quadrotor converges to the desired orientation within the prescribed time. □

Remark 4. *Based on Theorem 1, the proposed orientation observer guarantees sequential prescribed-time convergence from the leader to all followers under an LFF communication topology. Thus, the prescribed times should satisfy $T_{qj} < T_{qk} < T_{qi}$ for a quadrotor i with neighbors j and k ($j < k$).*

B. Bearing-only Formation Control Design

The distributed bearing-only formation control law is

$$\begin{aligned} \boldsymbol{u}_i = {} & k_{1,i} \sum\nolimits_{j\in\mathcal{N}_i} \hat{\boldsymbol{R}}_i^T (\bar{\boldsymbol{g}}_{ij} - \bar{\boldsymbol{g}}_{ij}^*) + k_{2,i} \sum\nolimits_{j\in\mathcal{N}_i} \dot{\boldsymbol{s}}_{1,i} \\ & + k_{3,i} \sum\nolimits_{j\in\mathcal{N}_i} \hat{\boldsymbol{R}}_i^T \bar{\boldsymbol{P}}_{ij} \hat{\boldsymbol{R}}_i \mathrm{sgn}(\dot{\boldsymbol{s}}_{1,i}) \end{aligned} \tag{8}$$

where $k_{1,i}, k_{2,i}, k_{3,i} \in \mathbb{R}^+$ are the controller parameters, $\bar{\boldsymbol{P}}_{ij} = \boldsymbol{I}_3 - \bar{\boldsymbol{g}}_{ij}\bar{\boldsymbol{g}}_{ij}^T = \boldsymbol{R}(\boldsymbol{q}_r)\boldsymbol{P}_{ij}\boldsymbol{R}^T(\boldsymbol{q}_r)$.

Motivated by [27], $\boldsymbol{s}_{1,i}$ are given by the following finite-time differentiator:

$$\begin{cases} \dot{\boldsymbol{s}}_{1,i} = -\lambda_1 \,\mathrm{sgn}^{1/2}\left(\boldsymbol{s}_{1,i} - \sum_{j\in\mathcal{N}_i} \hat{\boldsymbol{R}}_i^T \left(\bar{\boldsymbol{g}}_{ij} - \bar{\boldsymbol{g}}_{ij}^*\right)\right) + \boldsymbol{s}_{2,i} \\ \dot{\boldsymbol{s}}_{2,i} = -\lambda_2 \,\mathrm{sgn}\left(\boldsymbol{s}_{2,i} - \dot{\boldsymbol{s}}_{1,i}\right) \end{cases} \tag{9}$$

where $\boldsymbol{s}_{1,i}, \boldsymbol{s}_{2,i} \in \mathbb{R}^3$ are the states of the differentiator. According to [27], $\boldsymbol{s}_{1,i}$ converges to $\sum_{j\in\mathcal{N}_i} \hat{\boldsymbol{R}}_i^T (\bar{\boldsymbol{g}}_{ij} - \bar{\boldsymbol{g}}_{ij}^*)$ in finite-time $T_{si} > T_{qi}$ as long as the parameters $\lambda_1, \lambda_2 \in \mathbb{R}^+$ are properly selected.

Prior to the stability analysis, the following useful lemma is given:

Lemma 3. *[14] Consider a group of n agents with LFF structure, for the follower i and $j \in \mathcal{N}_i$, if $\boldsymbol{p}_i \neq \boldsymbol{p}_j$ holds for all $(i, j) \in \mathcal{E}$, then it yields that $\sum_{j\in\mathcal{N}_i} \boldsymbol{e}_{ij}^T(\boldsymbol{g}_{ij} - \boldsymbol{g}_{ij}^*) \geq 0$*

Theorem 2. *Suppose that Assumption 1-3 hold, the proposed control law (8) with (9) ensures that the position tracking error $\boldsymbol{e}_{pi}$ and velocity tracking error $\boldsymbol{e}_{vi}$ for follower quadrotor i ($3 \leq i \leq n$) converge to zero asymptotically if $k_{1,i}, k_{2,i} \in \mathbb{R}^+$ and $k_{3,i} > (\xi_a + \xi_d)/(1 - \boldsymbol{g}_{ij}^T \boldsymbol{g}_{ik})$.*

IEEE Robotics and Automation Letters (RA-L) paper, presented at ICRA 2026, Vienna, Austria. Cite as RA-L paper.

Proof. The proof of Theorem 2 is performed using mathematical induction. We firstly consider the third quadrotor ($i = 3$), which has the leader ($j = 1$) and first follower ($k = 2$) as its neighbors.

On the basis of lemma 3, we consider the Lyapunov function candidate $V_i = k_{1,i}\sum_{j\in\mathcal{N}_i} \boldsymbol{e}_{ij}^T(\boldsymbol{g}_{ij} - \boldsymbol{g}_{ij}^*) + \frac{1}{2}\boldsymbol{e}_{vi}^T\boldsymbol{e}_{vi}$. Since that close-loop system is nonsmooth, the stability theory for discontinuous system is employed for the following analysis [28], which implies that $\dot{V}_i \in^{a.e.} \dot{\tilde{V}}_i = \bigcap_{\varpi\in\partial V_i} \varpi^T K[\dot{\boldsymbol{v}}] = \nabla {V_i}^T K[\dot{\boldsymbol{v}}]$. Considering that $\boldsymbol{e}_{ij}^T\dot{\boldsymbol{g}}_{ij} = 0$, $\dot{\tilde{V}}_i$ is given as

$$\begin{aligned}\dot{\tilde{V}}_i &= k_{1,i}\sum_{j\in\mathcal{N}_i} \dot{\boldsymbol{e}}_{ij}^T(\boldsymbol{g}_{ij} - \boldsymbol{g}_{ij}^*) + k_{1,i}\sum_{j\in\mathcal{N}_i} \boldsymbol{e}_{ij}^T\dot{\boldsymbol{g}}_{ij} + \boldsymbol{e}_{vi}^T\dot{\boldsymbol{e}}_{vi} \\ &= k_{1,i}\sum_{j\in\mathcal{N}_i} \dot{\boldsymbol{e}}_{ij}^T(\boldsymbol{g}_{ij} - \boldsymbol{g}_{ij}^*) + \boldsymbol{e}_{vi}^T(K[\boldsymbol{u}_i] + \boldsymbol{d}_i - \dot{\boldsymbol{v}}^*)\end{aligned} \tag{10}$$

As $\boldsymbol{v}_i^* = \boldsymbol{v}_j^* = \boldsymbol{v}^*$ in the formation translates , it can be derived that $\dot{\boldsymbol{e}}_{ij} = \boldsymbol{p}_j - \boldsymbol{p_i} = \boldsymbol{e}_{vj} - \boldsymbol{e}_{vi} = -\boldsymbol{e}_{vi}$. Denoting the oth term ($o \in \{\mathrm{I}, \mathrm{II}\}$) of $\dot{\tilde{V}}_i$ as $\dot{\tilde{V}}_i^o$, (10) can be further transformed as

$$\dot{\tilde{V}}_i^{\mathrm{I}} = -k_{1,i}\sum_{j\in\mathcal{N}_i} {\boldsymbol{e}_{vi}}^T(\boldsymbol{g}_{ij} - \boldsymbol{g}_{ij}^*) \tag{11a}$$

$$\begin{aligned}\dot{\tilde{V}}_i^{\mathrm{II}} = \boldsymbol{e}_{vi}^T(k_{1,i}\sum_{j\in\mathcal{N}_i} \hat{\boldsymbol{R}}_i^T(\bar{\boldsymbol{g}}_{ij} - \bar{\boldsymbol{g}}_{ij}^*) + k_{2,i}\sum_{j\in\mathcal{N}_i} \dot{\boldsymbol{s}}_{1,i} \\ + k_{3,i}\sum_{j\in\mathcal{N}_i} \boldsymbol{P}_{ij}\mathrm{sgn}(\dot{\boldsymbol{s}}_{1,i}) + \boldsymbol{d}_i - \dot{\boldsymbol{v}}^*)\end{aligned} \tag{11b}$$

Considering that $\boldsymbol{e}_{vj} = \boldsymbol{0}$, The derivative of $\dot{V}_i^{\mathrm{I}}$ can be simplified as $\dot{V}_i^{\mathrm{I}} = -k_{1,i}\sum_{j\in\mathcal{N}_i} {\boldsymbol{e}_{vi}}^T(\boldsymbol{g}_{ij} - \boldsymbol{g}_{ij}^*)$. According to the orientation estimation, it can be derived that $\hat{\boldsymbol{R}}_i\bar{\boldsymbol{g}}_{ij} = \boldsymbol{g}_{ij}$ in $t \in [T_{qi}, +\infty)$. Recalling that $\boldsymbol{s}_{1,i} = \sum_{j\in\mathcal{N}_i} \hat{\boldsymbol{R}}_i^T(\bar{\boldsymbol{g}}_{ij} - \bar{\boldsymbol{g}}_{ij}^*)$ in $t \in [T_{si}, +\infty)$, $\dot{V}_i^{\mathrm{II}}$ can be calculated as $\dot{V}_i^{\mathrm{II}} = k_{1,i}\sum_{j\in\mathcal{N}_i} \boldsymbol{e}_{vi}^T(\boldsymbol{g}_{ij} - \boldsymbol{g}_{ij}^*) + k_{2,i}\sum_{j\in\mathcal{N}_i} \boldsymbol{e}_{vi}^T\dot{\boldsymbol{g}}_{ij} + k_{3,i}\sum_{j\in\mathcal{N}_i} \boldsymbol{e}_{vi}^T\boldsymbol{P}_{ij}\mathrm{sgn}(\dot{\boldsymbol{g}}_{ij}) + \boldsymbol{e}_{vi}^T\boldsymbol{d}_i - \boldsymbol{e}_{vi}^T\dot{\boldsymbol{v}}^*$. From $\dot{V}_i^{\mathrm{I}}$ and $\dot{V}_i^{\mathrm{II}}$, we have

$$\begin{aligned}\dot{V}_i &= -k_{2,i}\sum_{j\in\mathcal{N}_i} \boldsymbol{e}_{vi}^T\frac{\boldsymbol{P}_{ij}}{\|\boldsymbol{e}_{ij}\|}\boldsymbol{e}_{vi} + \boldsymbol{e}_{vi}^T\boldsymbol{d}_i - \boldsymbol{e}_{vi}^T\dot{\boldsymbol{v}}^* \\ &\quad - k_{3,i}\sum_{j\in\mathcal{N}_i} \boldsymbol{e}_{vi}^T\boldsymbol{P}_{ij}\mathrm{sgn}(\boldsymbol{P}_{ij}\boldsymbol{e}_{vi}) \\ &\le -k_{2,i}\sum_{j\in\mathcal{N}_i} \boldsymbol{e}_{vi}^T\frac{\boldsymbol{P}_{ij}}{\|\boldsymbol{e}_{ij}\|}\boldsymbol{e}_{vi} + \|\boldsymbol{e}_{vi}\|\|\boldsymbol{d}_i\| \\ &\quad + \|\boldsymbol{e}_{vi}\|\|\dot{\boldsymbol{v}}^*\| - k_{3,i}\sum_{j\in\mathcal{N}_i} \|\boldsymbol{P}_{ij}\boldsymbol{e}_{vi}\|_1 \\ &\le -k_{2,i}\sum_{j\in\mathcal{N}_i} \boldsymbol{e}_{vi}^T\frac{\boldsymbol{P}_{ij}}{\|\boldsymbol{e}_{ij}\|}\boldsymbol{e}_{vi} + (\xi_a + \xi_d)\|\boldsymbol{e}_{vi}\| \\ &\quad - k_{3,i}\sum_{j\in\mathcal{N}_i} \|\boldsymbol{P}_{ij}\boldsymbol{e}_{vi}\|_2 \\ &\le -k_{2,i}\sum_{j\in\mathcal{N}_i} \boldsymbol{e}_{vi}^T\frac{\boldsymbol{P}_{ij}}{\|\boldsymbol{e}_{ij}\|}\boldsymbol{e}_{vi} + (\xi_a + \xi_d)\|\boldsymbol{e}_{vi}\| \\ &\quad - k_{3,i}\lambda_{\min}\Big(\sum_{j\in\mathcal{N}_i} \boldsymbol{P}_{ij}\Big)\|\boldsymbol{e}_{vi}\|\end{aligned} \tag{12}$$

It can be easily deduced that $\sum_{j\in\mathcal{N}_i} \boldsymbol{P}_{ij}$ is positive semi-definite, with $\lambda_{\min}\left(\sum_{j\in\mathcal{N}_i} \boldsymbol{P}_{ij}\right) = 1 - |\boldsymbol{g}_{ij}^T\boldsymbol{g}_{ik}| = 0 \Leftrightarrow \boldsymbol{g}_{ij} \parallel \boldsymbol{g}_{ik}$. Before moving forward, we need to exclude $1 - |\boldsymbol{g}_{ij}^T\boldsymbol{g}_{ik}| = 0$ by showing that the set $\mathcal{S} = \left\{(\boldsymbol{p}, \boldsymbol{v}) | \boldsymbol{g}_{ij} \parallel \boldsymbol{g}_{ik}\right\}$ does not belong to any invariant set.

Suppose, for contradiction, that $\mathcal{S} = \{(\boldsymbol{p}, \boldsymbol{v}) \mid \exists i, j, k : \boldsymbol{g}_{ij} \times \boldsymbol{g}_{ik} = \boldsymbol{0}\}$ is invariant. Then $\boldsymbol{g}_{ij} \parallel \boldsymbol{g}_{ik}$ holds for all time, which implies $\dot{\boldsymbol{g}}_{ij} = \dot{\boldsymbol{g}}_{ik} = \boldsymbol{0}$. Since $\dot{\boldsymbol{g}}_{ij} = \frac{P_{ij}(\boldsymbol{v}_j - \boldsymbol{v}_i)}{\|\boldsymbol{p}_j - \boldsymbol{p}_i\|}$, this leads to $\boldsymbol{v}_j - \boldsymbol{v}_i \parallel \boldsymbol{g}_{ij}$. However, the first term of the control law is nonzero unless $\boldsymbol{g}_{ij} = \boldsymbol{g}_{ij}^*$ for all $j \in \mathcal{N}_i$. Note that $\boldsymbol{g}_{ij}^*$ and $\boldsymbol{g}_{ik}^*$ are designed to be not collinear under LFF structure, in other words, the system cannot remain in the state set $\mathcal{S}$.

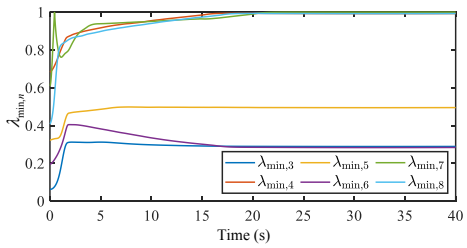

Fig. 3. $\lambda_{\min}$ of each follower in simulation scenario as Section IV.

Based on the above analysis, we have $\dot{V}_i \le 0$ if $k_{3,i} > (\xi_a + \xi_d)/(1 - |\boldsymbol{g}_{ij}^T\boldsymbol{g}_{ik}|)$ Therefore, it can be deduced from V_i that $\boldsymbol{e}_{ij}(\boldsymbol{g}_{ij} - \boldsymbol{g}_{ij}^*)$ and $\boldsymbol{e}_{vi}$ are bounded. Thus $\boldsymbol{e}_{pi}$ and $\boldsymbol{e}_{vi}$ converge to a compact set when $\dot{V}_i = 0$, which leads to two cases.

Case 1: $\boldsymbol{g}_{ij} = \boldsymbol{g}_{ij}^*$ and $\dot{\boldsymbol{g}}_{ij} = \boldsymbol{0}$, which proves that Theorem 2 holds for quadrotor i; Case 2: $\boldsymbol{g}_{ij} \neq \boldsymbol{g}_{ij}^*$ and $\dot{\boldsymbol{g}}_{ij} = \boldsymbol{0}$. Then the control input $\boldsymbol{u}_i$ continues to change $\boldsymbol{v}_i$. The velocity tracking error $\boldsymbol{e}_{vi} \to \infty$ and contradicts to $\boldsymbol{e}_{vi} = \boldsymbol{0}$. Thus, only Case 1 is appropriate.

Based on the LFF structure, we consider the follower quadrotor i with neighbors j and k. According to the mathematical induction, it is assumed that Theorem 2 holds for UAV o ($3 \le o \le i$) , which means that the formation tracking error of the neighbors of UAV i converges to zero asymptotically. Similar to the above proof, it can be concluded that Theorem 2 holds for all follower quadrotors i ($3 \le i \le n$). By the uniqueness of the LFF structure [24], if $\boldsymbol{g}_{ij} = \boldsymbol{g}_{ij}^*$ holds for $(i, j) \in \mathcal{E}$, it yields that $\boldsymbol{p}_i = \boldsymbol{p}_i^*$. Consequently, the desired formation configuration is achieved. □

Remark 5. *Although the bearing vectors $\boldsymbol{g}_{ij}(t)$ and $\boldsymbol{g}_{ik}(t)$ are time-varying, Theorem 2 guarantees their asymptotic convergence to the desired values $\boldsymbol{g}_{ij}^*$ and $\boldsymbol{g}_{ik}^*$. Since $(\boldsymbol{g}_{ij}^*)^T\boldsymbol{g}_{ik}^* < 1$ holds under the non-collinearity condition, there exists a time constant $T > 0$ such that, for all $t > T$, $\left|\boldsymbol{g}_{ij}^T(t)\boldsymbol{g}_{ik}(t)\right| \le \left|(\boldsymbol{g}_{ij}^*)^T\boldsymbol{g}_{ik}^*\right| + \delta(T) < 1$, where $\delta(T) > 0$ is a small error term that monotonically decreases as T increases. This implies that, for sufficiently large t, $1 - \left|\boldsymbol{g}_{ij}^T\boldsymbol{g}_{ik}\right|$ is lower-bounded by a positive constant $\lambda_i^{\min} = 1 - \left|(\boldsymbol{g}_{ij}^*)^T\boldsymbol{g}_{ik}^*\right| - \delta(T) > 0$. Based on this lower bound, the gain condition can be conservatively determined as $k_{3,i} > (\xi_a + \xi_d)/\lambda_i^{\min}$, where $\lambda_i^{\min}$ can be selected using the desired bearing vectors $\boldsymbol{g}_{ij}^*$, $\boldsymbol{g}_{ik}^*$, and $\delta(T)$.*

Remark 6. *In practice, $\lambda_i^{\min}$ can be conservatively chosen using the initial value of $1 - \left|\boldsymbol{g}_{ij}^T\boldsymbol{g}_{ik}\right|$, which ensures the gain condition holds during the entire system evolution. It is worth noting that obtaining a closed-form expression for $\delta(T)$ and a strict uniform bound remains an open problem. Nevertheless, numerical simulations (see Fig. 3) confirm that $1 - \left|\boldsymbol{g}_{ij}^T\boldsymbol{g}_{ik}\right|$ monotonically converges to its asymptotic value, and its minimum occurs at the initial time. This observation supports the proposed conservative gain selection strategy.*

IEEE Robotics and Automation Letters (RA-L) paper, presented at ICRA 2026, Vienna, Austria. Cite as RA-L paper.

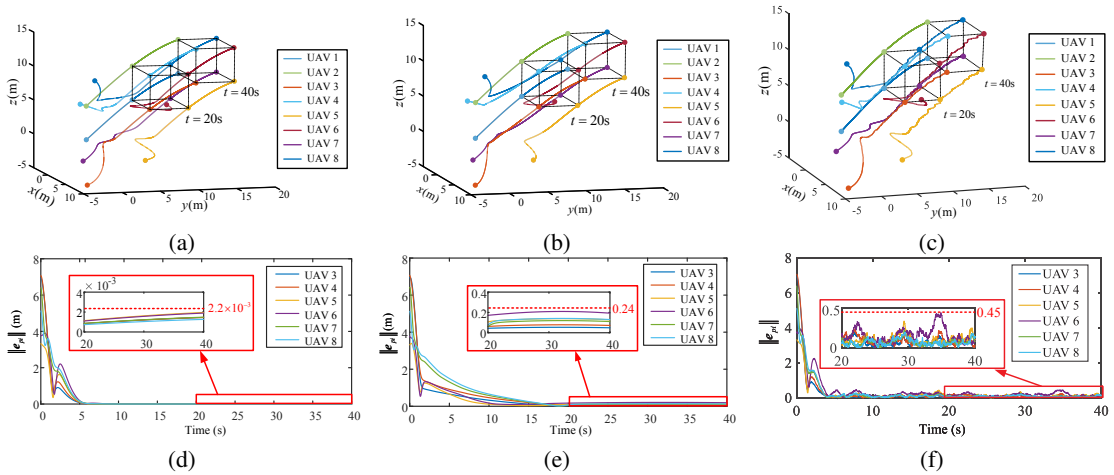

Fig. 4. Formation trajectories and tracking errors $\|\boldsymbol{e}_{pi}\|$ under (a,d) the proposed method, (b,e) the method in [18], and (c,f) bearing noise and intermittent visibility.

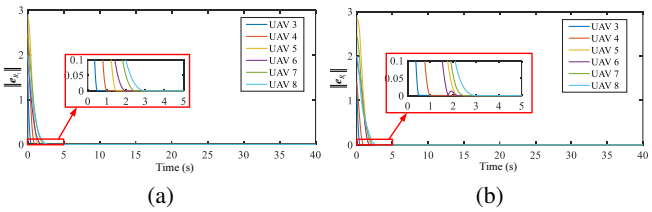

Fig. 5. Orientation estimation errors $\|\boldsymbol{e}_{Ri}\|$: (a) nominal case; (b) mismatched case.

IV. Simulations

In this section, numerical simulations are carried out to validate the performance of the proposed formation control law for quadrotor swarm. Besides, some comparisons with existing bearing-only formation control scheme are presented.

A. Bearing-only formation maneuvering control

In the simulation scenario, a group of 8 quadrotors with LFF structure are considered, as illustrated in Fig. 1a. The desired formation configuration is a cube with side length of 5m. The initial positions are given as $\boldsymbol{p}_1 = [0,0,0]^T, \boldsymbol{p}_2 = [0,0,5]^T, \boldsymbol{p}_3 = [9,-4,-4]^T, \boldsymbol{p}_4 = [9,-5,8]^T, \boldsymbol{p}_5 = [8,4,-1]^T, \boldsymbol{p}_6 = [7.5,7,7]^T, \boldsymbol{p}_7 = [-4,3,7.5]^T, \boldsymbol{p}_8 = [-4,3,7.5]^T$. The initial velocity $\boldsymbol{v}_i(0) \in \mathbb{R}^3$ is randomly generated with each component uniformly distributed within $[-1,1]$ m/s. The initial orientation $\boldsymbol{q}_i(0)$ and its estimate $\hat{\boldsymbol{q}}_i(0)$ are randomly generated such that their corresponding Euler angles are uniformly distributed within $(-10°, 10°)$. The disturbance is set as $\boldsymbol{d}_i = [0.2\sin 0.12t, 0.15\cos 0.2t, 0.1\sin 0.18t]^T$.

To evaluate the performance of the proposed bearing-only control law, the time-varying velocities for the leader and first follower are set as $\boldsymbol{v}^* = [0, 0.3, 0.3\cos 0.03t]^T$ m/s, the orientation of the leader and first follower are set as $\boldsymbol{R}^* = \boldsymbol{I}_3$. The parameters of the orientation estimator are set as $a_i = 2$ and $b_i = 5$. The prescribed convergence time vector $\boldsymbol{T}_q = [T_{q3}, T_{q4}, \cdots, T_{q8}]^T = [0.5, 1, 1.5, 2, 2.5, 3]^T$s. The parameters of the controller are set as $k_{1,i} = 15, k_{2,i} = 15, k_{3,i} = 8$. The parameters of the differentiator are set as $\lambda_1 = 2, \lambda_2 = 3$.

The simulation results are shown in Fig. 4a–5a. Figure 4a illustrates that the formation is achieved within 20,s and translates as desired. The orientation and position tracking errors are defined as $\|\boldsymbol{e}_{Ri}\| = \left\|\hat{\boldsymbol{R}}_i - \boldsymbol{R}_i^*\right\|$ and $\|\boldsymbol{e}_{pi}\| = \|\boldsymbol{p}_i - \boldsymbol{p}_i^*\|$, respectively. As shown in Fig. 5a, the orientation estimation error converges to zero within the prescribed convergence time $\boldsymbol{T}_q$ and remains zero afterwards. Figure 4d demonstrates that the formation tracking error of the follower quadrotors also converges to and maintains zero throughout formation maneuvering.

To emulate realistic onboard sensing, zero-mean Gaussian noise with a variance of 0.05 is added to the followers' bearing measurements. For UAV 6, intermittent visibility is additionally modeled by a Bernoulli process with an invisibility probability of 0.2 to simulate occlusion or sensor failure. As shown in Fig. 4c and Fig. 4f, the UAV trajectories and tracking errors exhibit slight fluctuations but remain within acceptable accuracy. UAV 6 shows the largest error due to visibility loss but quickly recovers once visibility is restored. Overall, although measurement noise and intermittent visibility degrade performance, the formation remains stable, highlighting the need for improved robustness in future work.

To assess the robustness to convergence-time mismatch in orientation estimation, an additional simulation is conducted, wherein the prescribed orientation estimation convergence time of UAV 5 is deliberately delayed to 2.2 s, while the convergence time of downstream UAVs 6 and 7 are set as 2.0 s and 2.5 s. As shown in Fig. 5b, potential delay in the estimation time of UAV 5 leads to slight fluctuations in UAV 6's estimation around the 2.0 s. In addition, since UAV 6 still converges before 2.5 s, UAV 7 and UAV 8 remains unaffected. Since the orientation estimation is achieved faster than the formation tracking, the mismatched convergence of orientation estimation does not affect the formation stability.

IEEE Robotics and Automation Letters (RA-L) paper, presented at ICRA 2026, Vienna, Austria. Cite as RA-L paper.

TABLE I
EXPERIMENT PARAMETERS.

Parameter	Value
RTK measurement frequency	5 Hz
Mass of the quadrotor	686 g
Maximum lift force	16.562 N
Orientation estimation gain	$a_i = 5$, $b_i = 7.5$
Prescribed time for orientation estimation	$\boldsymbol{T}_q = [0.5,\ 1,\ 1.5,\ 2]^T$ s
Controller gain	$k_{1,i} = k_{2,i} = 10$, $k_{3,i} = 9$
Differentiator gain	$\lambda_1 = \lambda_2 = 5$
Bearing-rate filter cut-off frequency	2 Hz

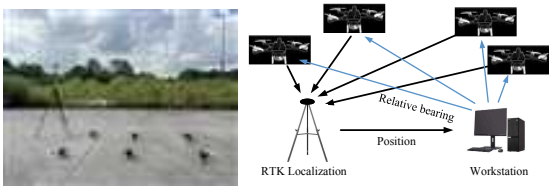

(a) (b)

Fig. 6. (a) A snapshot of the experiment platform. (b) Configuration of the experiment platform.

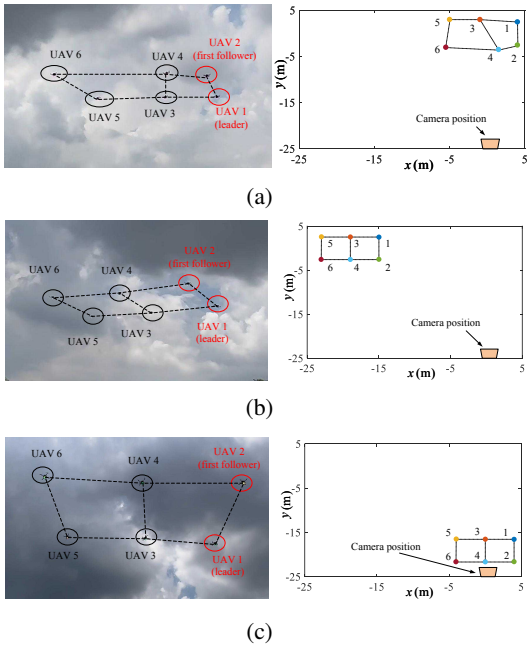

(a)

(b)

(c)

Fig. 7. The snapshots and positions of the quadrotors at (a) $t = 0$, (b) $t = 20$s, and (c) $t = 40$s

B. Comparisons with existing works

To evaluate the effectiveness of the proposed control scheme, we compare it with the method in [18]. The formation configuration, sensing topology, and initial conditions are kept the same as in Section IV-A. The control parameters are set to $k_1 = 6$, $k_2 = 5$, and $k_3 = 12$. Since the method in [18] requires the desired acceleration to be shared among quadrotors, $\dot{\boldsymbol{v}}^*$ is computed from $\dot{\boldsymbol{p}}^*$ accordingly.

Fig. 4b and Fig. 4e show the simulation results using the method proposed in [18]. The trajectories in Fig. 4b demonstrate that the method can achieve the desired formation. However, as shown in Fig. 4e, the formation tracking error remains significantly larger compared to our method, highlighting its limited robustness under time-varying velocity and disturbances.

V. EXPERIMENT VALIDATION

A. Experimental Setup and Results

To further assess the performance of the proposed method, outdoor experiment is performed on a group of 6 quadrotors with communication topology illustrated in Fig. 1b. To suppress high-frequency noise from the RTK station, a first-order low-pass filter is applied to the estimated bearing-rate signals before differentiation. The implementation parameters are presented as Table I.

Fig. 9 compares the raw and filtered signals for a representative agent. A feedback linearization algorithm is employed to convert the UAV dynamics into a double integrator model. As shown in Fig. 6, the experimental setup uses a ZED-F9R module for RTK localization, with relative bearings computed on a workstation and transmitted to each UAV via 5.8 GHz Wi-Fi.

In the experiment, the UAVs form a rectangle in a horizontal plane. They first take off to 12 m and reach initial positions

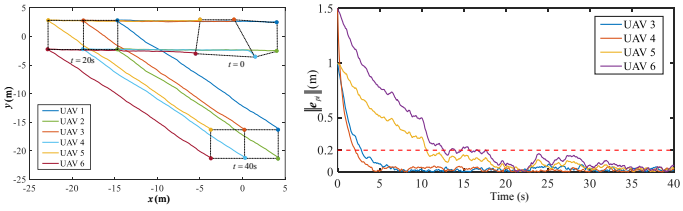

(a) (b)

Fig. 8. (a) Formation trajectories and (b) Formation tracking error $\|\boldsymbol{e}_{pi}\|$ of the quadrotors in the experiment

randomly distributed around the desired formation. The swarm moves along the negative x-direction to achieve the formation within 20 s, then translates diagonally toward the positive x- and negative y-directions while maintaining the formation for $t \in (20, 40]$ s. The desired speeds are 1 m/s for $t \in [0, 20]$ s and 1.414 m/s for $t \in (20, 40]$ s.

The experimental results are shown in Fig. 7–8. Figure 7 presents snapshots of the quadrotors during the maneuver and their positions relative to the camera. The trajectories in Fig. 8a show that the formation is achieved within 20 s and maintained during motion. Figure 8b illustrates that the formation tracking errors converge to a bounded set, validating the effectiveness of the proposed control strategy.

B. Discussions

In the experiments, an RTK-based localization system was used to obtain relative bearing measurements due to limitations in onboard sensing and computational resources. Although cameras and UWB modules are available, they are prone to distortion, noise, occlusion, latency, and non-line-of-sight effects [29], which can degrade bearing accuracy and risk violating connectivity. The RTK system provides a practical

IEEE Robotics and Automation Letters (RA-L) paper, presented at ICRA 2026, Vienna, Austria. Cite as RA-L paper.

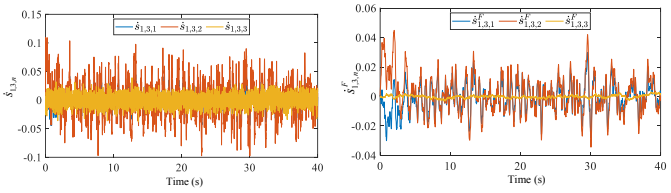

(a) (b)

Fig. 9. Profiles of (a) the raw signal $\dot{\boldsymbol{s}}_{1,3}$ and (b) the filtered signal $\dot{\boldsymbol{s}}^F_{1,3}$

compromise for validating the proposed method, consistent with prior studies [11], [14], [19].

It should be noted that the experiments were conducted at low speeds for safety and environment constraints. At higher speeds, linearized dynamics may introduce errors and cascaded bearing control may experience lag. Integrating the method with realistic onboard sensing and high-speed flight remains a relevant challenge for future work, including improving measurement accuracy, control robustness, and systematic performance analysis under aggressive conditions.

VI. Conclusion

In this paper, the bearing-only formation maneuvering control problem of quadrotors in local coordinates is addressed. A cascaded control framework integrating a distributed prescribed-time orientation estimator and a bearing-based formation controller is developed. The proposed approach eliminates the need for global orientation measurements and guarantees convergence of formation tracking errors under time-varying desired velocities and external disturbances. Its effectiveness is validated through both simulations and experiments.

References

[1] J. Hu, H. Niu, J. Carrasco, B. Lennox, and F. Arvin, "Fault-tolerant cooperative navigation of networked uav swarms for forest fire monitoring," *Aerosp. Sci. Technol.*, vol. 123, p. 107494, 2022.

[2] Y. Liu, F. Zhang, P. Huang, and X. Zhang, "Analysis, planning and control for cooperative transportation of tethered multi-rotor uavs," *Aerosp. Sci. Technol.*, vol. 113, p. 106673, 2021.

[3] L. Briñón-Arranz, A. Renzaglia, and L. Schenato, "Multirobot symmetric formations for gradient and hessian estimation with application to source seeking," *IEEE Trans. Robot.*, vol. 35, no. 3, pp. 782–789, 2019.

[4] J. Wang, L. Han, X. Dong, Q. Li, and Z. Ren, "Distributed sliding mode control for time-varying formation tracking of multi-uav system with a dynamic leader," *Aerosp. Sci. Technol.*, vol. 111, p. 106549, 2021.

[5] F. Sahebsara and M. de Queiroz, "On the stability of distance-based formation control with minimally globally rigid graphs," *Syst. Control Lett.*, vol. 185, p. 105726, 2024.

[6] Y. Zhang, S. Wang, X. Wang, and X. Tian, "Bearing-based formation control for multiple underactuated autonomous surface vehicles with flexible size scaling," *Ocean Eng.*, vol. 267, p. 113242, 2023.

[7] Y. Zhang, S. Oğuz, S. Wang, E. Garone, X. Wang, M. Dorigo, and M. K. Heinrich, "Self-reconfigurable hierarchical frameworks for formation control of robot swarms," *IEEE T. Cybern.*, vol. 54, no. 1, pp. 87–100, 2023.

[8] S. Zhao and D. Zelazo, "Bearing rigidity and almost global bearing-only formation stabilization," *IEEE Trans. Autom. Control*, vol. 61, no. 5, pp. 1255–1268, 2015.

[9] S. Li, S. Wang, X. Wang, and Y. Zhang, "Bearing-only prescribed-time formation control of uav swarm with external disturbance," in *2023 IEEE 18th Conference on Industrial Electronics and Applications (ICIEA)*. IEEE, 2023, pp. 1702–1707.

[10] S. Li, X. Wang, S. Wang, and Y. Zhang, "Distributed bearing-only formation control for uav-uwsv heterogeneous system," *Drones*, vol. 7, no. 2, p. 124, 2023.

[11] Z. Li, H. Tnunay, S. Zhao, W. Meng, S. Q. Xie, and Z. Ding, "Bearing-only formation control with prespecified convergence time," *IEEE T. Cybern.*, vol. 52, no. 1, pp. 620–629, 2020.

[12] S. Li, S. Wang, Y. Zhang, X. Wang, Y. Zhang, W. Wu, R. Chen, and R. Mu, "Distributed bearing-based fault-tolerant formation control of fixed-wing uav swarm with prescribed performance," *Aerosp. Sci. Technol.*, p. 110897, 2025.

[13] M. H. Trinh and H.-S. Ahn, "Finite-time bearing-based maneuver of acyclic leader-follower formations," *IEEE Control Syst. Lett.*, vol. 6, pp. 1004–1009, 2021.

[14] S. Zhao, Z. Li, and Z. Ding, "Bearing-only formation tracking control of multiagent systems," *IEEE Trans. Autom. Control*, vol. 64, no. 11, pp. 4541–4554, 2019.

[15] Z. Song, M. Xie, and H. Huang, "Bearing-only formation tracking control for multi-agent systems with time-varying velocity leaders," *IEEE Control Syst. Lett.*, 2024.

[16] J. Zhao, X. Yu, X. Li, and H. Wang, "Bearing-only formation tracking control of multi-agent systems with local reference frames and constant-velocity leaders," *IEEE Control Syst. Lett.*, vol. 5, no. 1, pp. 1–6, 2020.

[17] C. Garanayak and D. Mukherjee, "Bearing-only formation control with bounded disturbances in agents' local coordinate frames," *IEEE Control Syst. Lett.*, 2023.

[18] Q. Lin, Z. Miao, Y. Chen, X. Wang, W. He, and Y. Wang, "Bearing-only formation maneuvering for uav swarm over directed interaction topologies," *IEEE T. Intell. Veh.*, 2024.

[19] K. Wu, J. Hu, Z. Ding, and F. Arvin, "Finite-time fault-tolerant formation control for distributed multi-vehicle networks with bearing measurements," *IEEE Trans. Autom. Sci. Eng.*, vol. 21, no. 2, pp. 1346–1357, 2023.

[20] I. Mas and C. Kitts, "Quaternions and dual quaternions: Singularity-free multirobot formation control," *J. Intell. Robot. Syst.*, vol. 87, pp. 643–660, 2017.

[21] X. Dong, Y. Zhou, Z. Ren, and Y. Zhong, "Time-varying formation tracking for second-order multi-agent systems subjected to switching topologies with application to quadrotor formation flying," *IEEE Trans. Ind. Electron.*, vol. 64, no. 6, pp. 5014–5024, 2016.

[22] S. Bertrand, N. Guénard, T. Hamel, H. Piet-Lahanier, and L. Eck, "A hierarchical controller for miniature vtol uavs: Design and stability analysis using singular perturbation theory," *Control Eng. Practice*, vol. 19, no. 10, pp. 1099–1108, 2011.

[23] B. Herissé, T. Hamel, R. Mahony, and F.-X. Russotto, "Landing a vtol unmanned aerial vehicle on a moving platform using optical flow," *IEEE Trans. Robot.*, vol. 28, no. 1, pp. 77–89, 2011.

[24] M. H. Trinh, S. Zhao, Z. Sun, D. Zelazo, B. D. Anderson, and H.-S. Ahn, "Bearing-based formation control of a group of agents with leader-first follower structure," *IEEE Trans. Autom. Control*, vol. 64, no. 2, pp. 598–613, 2018.

[25] Y. Zhu, Q. Guo, Y. Tang, X. Zhu, Y. He, H. Huang, and S. Luo, "Cfd simulation and measurement of the downwash airflow of a quadrotor plant protection uav during operation," *Comput. Electron. Agric.*, vol. 201, p. 107286, 2022.

[26] X. Li, Y. Zhu, X. Zhao, and J. Lu, "Bearing-based prescribed time formation tracking for second-order multi-agent systems," *IEEE Trans. Circuits Syst. II-Express Briefs*, vol. 69, no. 7, pp. 3259–3263, 2022.

[27] A. Levant, "Higher-order sliding modes, differentiation and output-feedback control," *Int. J. Control*, vol. 76, no. 9-10, pp. 924–941, 2003.

[28] D. Shevitz and B. Paden, "Lyapunov stability theory of nonsmooth systems," *IEEE Trans. Autom. Control*, vol. 39, no. 9, pp. 1910–1914, 1994.

[29] Y. Lv, Z. Wu, H. Zhang, Z. Wang, and H. Yan, "Local-bearing-based prescribed-time distributed localization of multiagent systems with noisy measurement," *IEEE Trans. Ind. Inform.*, vol. 20, no. 7, pp. 9518–9526, 2024.